Article

Neuron

Parallel *Pbx*-Dependent Pathways Govern the Coalescence and Fate of Motor Columns

Highlights

- Spinal motor neuron somatotopic organization requires *Pbx* gene function
- Removal of *Pbx* genes leads to a loss of all Hox-dependent MN subtypes
- Pbx proteins regulate a subset of genes independent of Hox transcription factors
- *Pbx* genes operate in parallel genetic pathways to govern MN columnar coalescence

Authors

Olivia Hanley, Rediet Zewdu, Lisa J. Cohen, ..., David H. Lee, Licia Selleri, Jeremy S. Dasen

Correspondence

jeremy.dasen@nyumc.org

In Brief

The organization of motor neurons into columnar groups is a defining feature of topographic maps in the CNS. Hanley et al. show that Pbx proteins, cofactors for Hox transcription factors, are essential for the coalescence of neurons within motor columns.

Accession Numbers

GSE84271

Hanley et al., 2016, Neuron *91*, 1005–1020
September 7, 2016
http://dx.doi.org/10.1016/j.neuron.2016.07.043

CellPress

Neuron
Article

Parallel *Pbx*-Dependent Pathways Govern the Coalescence and Fate of Motor Columns

Olivia Hanley,[1] Rediet Zewdu,[2] Lisa J. Cohen,[3] Heekyung Jung,[1] Julie Lacombe,[1] Polyxeni Philippidou,[1] David H. Lee,[1] Licia Selleri,[2] and Jeremy S. Dasen[1,*]
[1]Neuroscience Institute and Department of Neuroscience and Physiology, NYU School of Medicine, New York, NY 10016, USA
[2]Department of Cell and Developmental Biology, Weill Cornell Medical College, New York, NY 10065, USA
[3]Genome Technology Center, NYU Langone Medical Center, 550 First Avenue, New York, NY 10016, USA
*Correspondence: jeremy.dasen@nyumc.org
http://dx.doi.org/10.1016/j.neuron.2016.07.043

SUMMARY

The clustering of neurons sharing similar functional properties and connectivity is a common organizational feature of vertebrate nervous systems. Within motor networks, spinal motor neurons (MNs) segregate into longitudinally arrayed subtypes, establishing a central somatotopic map of peripheral target innervation. MN organization and connectivity relies on Hox transcription factors expressed along the rostrocaudal axis; however, the developmental mechanisms governing the orderly arrangement of MNs are largely unknown. We show that *Pbx* genes, which encode Hox cofactors, are essential for the segregation and clustering of neurons within motor columns. In the absence of *Pbx1* and *Pbx3* function, Hox-dependent programs are lost and the remaining MN subtypes are unclustered and disordered. Identification of Pbx gene targets revealed an unexpected and apparently Hox-independent role in defining molecular features of dorsally projecting medial motor column (MMC) neurons. These results indicate *Pbx* genes act in parallel genetic pathways to orchestrate neuronal subtype differentiation, connectivity, and organization.

INTRODUCTION

In many regions of the CNS, groups of neurons targeting common peripheral targets are centrally organized within topographic maps. The ordered spatial relationship between neuronal position and target specificity is a prominent anatomical feature of primary sensory and motor systems, including the retinotectal map of the visual system and the somatotopic representation of the body surface within the cortex (Kania, 2014; Levine et al., 2012). While topographical maps appear to be critical in establishing appropriate connectivity and functionality within neural circuits, the underlying genetic mechanisms governing their formation are poorly understood.

Within the vertebrate spinal cord, the cell bodies of motor neurons (MNs) innervating specific muscle targets are somatotopically organized within columnar, divisional, and pool subtypes (Lance-Jones and Landmesser, 1981; Landmesser, 1978a, 1978b; Romanes, 1951). The topographical arrangement of spinal MNs appears to be a unique attribute of vertebrate motor systems, as MN subtypes of invertebrates lack somatotopic organization, although MN dendrites in *Drosophila* are highly structured (Baek and Mann, 2009; Landgraf et al., 2003; Thor and Thomas, 2002). While the purpose of MN clustering in vertebrates is not fully understood, it likely evolved to simplify the task of coordinating limb muscle activation sequences during locomotion (Fetcho, 1987), acting in part by enabling and constraining MN access to specific premotor circuits (Goetz et al., 2015; Hinckley et al., 2015; Sürmeli et al., 2011).

An early step in establishing MN topographical organization involves the separation of dorsally and ventrally projecting subtypes along the mediolateral axis of the spinal cord. Neurons within the medial motor column (MMC) project dorsally to innervate axial muscles and occupy a ventromedial position. All other MN subtypes typically reside more laterally and initially pursue ventral trajectories. These highly diverse non-MMC populations are generated at specific segmental levels of the spinal cord as a consequence of *Hox* gene activity along the rostrocaudal axis (Philippidou and Dasen, 2013). At forelimb and hindlimb levels, a network of *Hox* genes specifies the identity of the lateral motor columns (LMCs) as well as its resident ~50 MN pools targeting individual limb muscles. At thoracic levels, the *Hoxc9* gene determines the identity of preganglionic motor column (PGC) neurons, and it contributes to the positioning of the hypaxial motor column (HMC) (Jung et al., 2010). In contrast MMC neurons are generated at all segmental levels and appear to differentiate in a Hox-independent manner (Dasen et al., 2003, 2008; Sharma et al., 1998).

The cell fate determinants that facilitate the clustering of MNs into columns are largely unknown. Mutation of the transcription factor *Pea3* leads to a disorganization of neurons within a subset of LMC pools (Livet et al., 2002). Downstream targets of Pea3 include type II cadherins, which appear to be critical for the clustering of neurons within motor pools. MN pools express specific cadherin profiles, and manipulating cadherin expression alters MN settling position (Price et al., 2002). Genetic removal of α- and γ-*catenin*, which mediate signal transduction through cadherins, leads to a disorganization of neurons within the LMC (Demireva et al., 2011). Nevertheless, the separation of MMC and non-MMC populations persists in the absence of

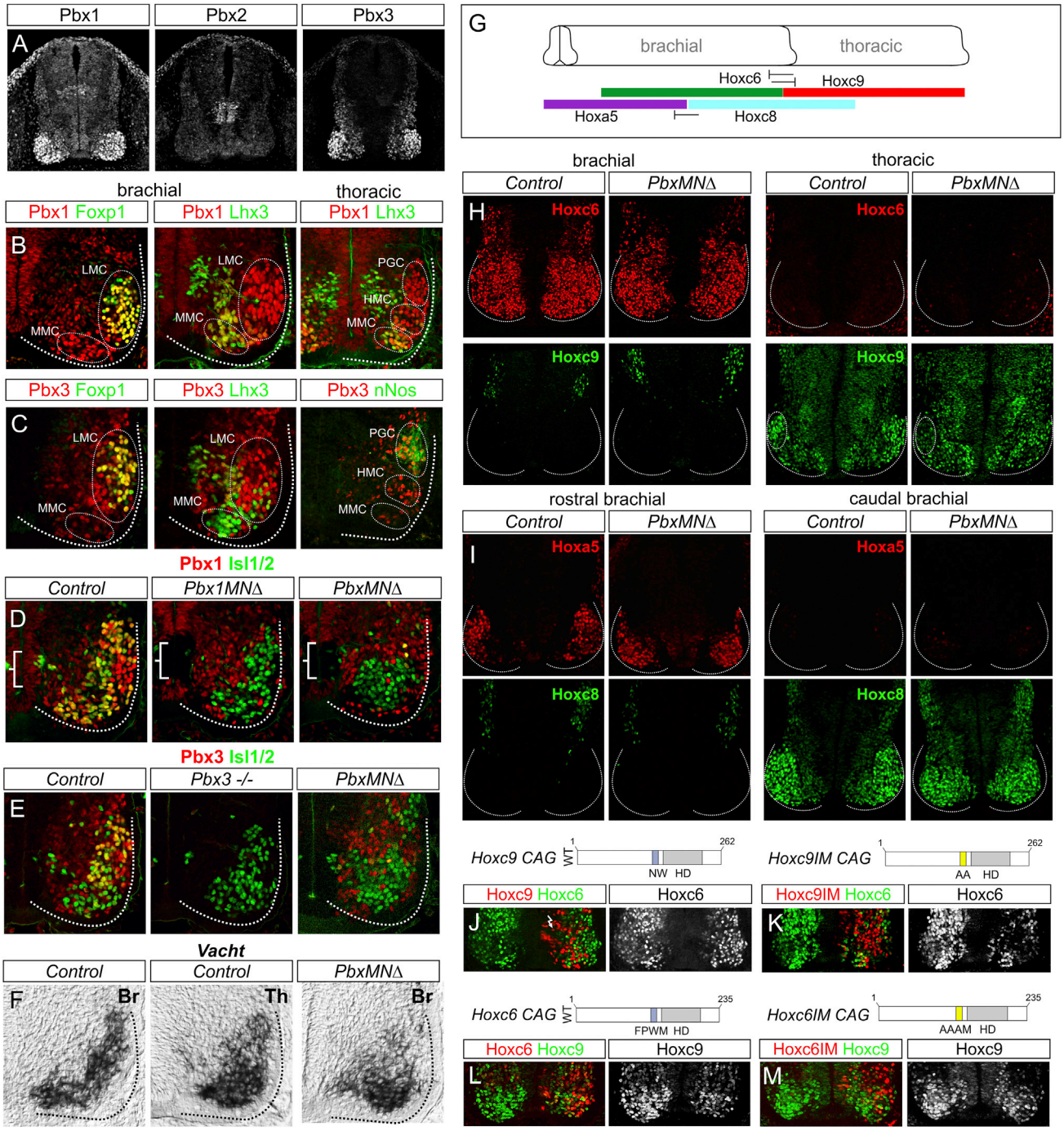

Figure 1. *Pbx* Genes Are Not Required for MN Generation or Establishing *Hox* Boundaries

(A) Pbx protein expression in mouse spinal cord at E11.5. Pbx1 is expressed in progenitors and postmitotic MNs. Pbx2 is expressed at low levels in progenitors and postmitotic neurons and a population of interneuron progenitors. Pbx3 is expressed by postmitotic spinal neurons.

(B) Pbx1 colocalizes with Foxp1^{+} LMC neurons at brachial levels, Lhx3^{+} MMC neurons, and thoracic HMC and PGC neurons.

(C) Pbx3 is restricted to rostral brachial Foxp1^{+} LMC neurons and excluded from Lhx3^{+} MMC neurons. At thoracic levels, Pbx3 is expressed in HMC and nNos^{+} PGC neurons.

(D) Pbx1 expression is lost in progenitors (brackets) and postmitotic MNs in *Pbx1*$^{MN\Delta}$ and *Pbx*$^{MN\Delta}$ mice.

(E) Pbx3 expression is lost in *Pbx3*$^{-/-}$ and *Pbx*$^{MN\Delta}$ mice. Pbx3 staining in *Pbx*$^{MN\Delta}$ section is from the *Pbx3* conditional allele.

(F) *Vacht* mRNA expression at E12.5 in control brachial (Br) and thoracic (Th) MNs and in Br MNs of *Pbx*$^{MN\Delta}$ mice. Loss of Br MNs in *Pbx* mutants does not appear to be due to increased apoptosis (Figure S1H).

(legend continued on next page)

Pea3 and *catenins*, suggesting an earlier program governs MN columnar organization.

Hox transcription factors are essential during MN subtype diversification and are plausible candidates for governing the coalescence and somatotopic organization of MMC and non-MMC populations. Disruption of *Hox* gene function, however, typically leads to a transformation of ventrally projecting MNs while preserving their separation from the MMC. For example, in mice mutant for the *Hoxc9* gene, thoracic level-specific motor columns are converted to an LMC fate, but the distribution and position of MMC neurons is unchanged (Jung et al., 2010). Similarly, the relative position of MMC and non-MMC neurons is retained after depletion of the *Foxp1* gene, which encodes an accessory factor required for Hox-dependent programs of LMC and PGC differentiation (Dasen et al., 2008; Rousso et al., 2008). Certain Hox activities in MNs are unaffected by *Foxp1* mutation, including the initial induction of the *Foxp1* gene and the cross-repressive interactions necessary to establish Hox expression boundaries (Dasen et al., 2008; Jung et al., 2014). The retention of early Hox function in *Foxp1* mutants raises the possibility that Hox-dependent pathways contribute to the segregation and clustering of spinal MNs.

We reasoned that insight into the contribution of subtype determinants during MN columnar topographic organization might emerge through manipulations that disrupt Hox activities but otherwise preserve basic features of MN class identity. Hox proteins are known to rely on interactions with both cell-type-restricted and broadly expressed cofactors (Mann et al., 2009; Moens and Selleri, 2006). In most cellular contexts, the three amino acid loop extension (TALE) class of homeodomain proteins plays prominent roles in shaping Hox protein specificity. Pbx proteins, vertebrate homologs of the *Drosophila* TALE protein extradenticle, are essential for Hox proteins to select gene targets with high affinity. Analysis of *Pbx* gene function has been constrained due to the existence of multiple gene homologs and the early lethality of mice lacking individual *Pbx* genes (Moens and Selleri, 2006). Nevertheless, studies in zebrafish and mice have demonstrated essential roles for *Pbx* genes in rostrocaudal patterning and cell type specification in the hindbrain (Cooper et al., 2003; Vitobello et al., 2011; Waskiewicz et al., 2002). Interpretation of these results is, however, confounded by a non-cell-autonomous role of *Pbx* genes in controlling the expression of morphogens during rhombomere development.

Here we investigated the role of *Pbx* genes in neuronal differentiation and topographical organization by selectively removing their activities from spinal MNs. We found that *Pbx* genes are essential for the specification and connectivity of Hox-dependent MN columnar, divisional, and pool subtypes. Unexpectedly, the remaining dorsally and ventrally projecting neurons were intermixed in *Pbx* mutants, indicating *Pbx* genes are also responsible for governing the basic program of MN clustering and columnar segregation. Identification of *Pbx* gene targets in MNs revealed an unanticipated Hox-independent role in defining molecular features of dorsally projecting MMC neurons. These findings indicate that *Pbx* genes operate in parallel MN subtype-specific pathways to govern the formation of spinal motor columns.

RESULTS

Pbx Genes Are Dispensable in Early MN Differentiation and Rostrocaudal Patterning

To assess the involvement of *Pbx* genes in MN subtype diversification, we first examined the profile of Pbx protein expression within the spinal cord. Three of the four mammalian Pbx proteins, Pbx1, Pbx2, and Pbx3, were expressed by spinal neurons at embryonic day (E)11.5 (Figure 1A). Pbx1 was ubiquitously expressed with elevated expression in progenitors and postmitotic MNs (Figures 1A, 1B, and S1A). Pbx2 was detected at low levels throughout the spinal cord, while Pbx3 was expressed in postmitotic neurons, with prominent expression in MNs (Figures 1A and 1C). Pbx3 also was restricted within Hox-dependent MN populations, including thoracic PGC neurons and subsets of limb-level LMC neurons, but was excluded from axially projecting MMC neurons (Figures 1C and S1B–S1D). Thus, in mice, two of the four mammalian Pbx proteins, Pbx1 and Pbx3, are highly expressed by spinal MNs.

To determine the role of *Pbx* genes in MN differentiation, we devised genetic strategies to inactivate their function. To circumvent the early lethality of *Pbx1*-null mutant mice (Selleri et al., 2001), we bred a floxed *Pbx1* allele to *Olig2*::*Cre* mice to generate an MN-specific knockout line (referred to henceforth as $Pbx1^{MN\Delta}$ mice) (Koss et al., 2012). *Pbx3* mutants are viable during embryogenesis (Rhee et al., 2004), and we therefore generated *Pbx1* and *Pbx3* double mutants by introducing a *Pbx3*-null line into the $Pbx1^{MN\Delta}$ background. The phenotypes of $Pbx1^{MN\Delta}$;$Pbx3^{-/-}$ mice were not enhanced by the introduction of a $Pbx2^{-/-}$ allele (data not shown) (Selleri et al., 2004), and we therefore refer to *Pbx1*/*Pbx3* double mutants as $Pbx^{MN\Delta}$ mice. In $Pbx1^{MN\Delta}$, $Pbx3^{-/-}$, and $Pbx^{MN\Delta}$ lines, the respective Pbx proteins were effectively depleted from MNs (Figures 1D and 1E), and, of these alleles, only a rare $Pbx1^{MN\Delta}$ mutant survived until adulthood. We also generated embryos in which both *Pbx1* and *Pbx3* were selectively eliminated from MNs by combining a floxed *Pbx3* allele (Rottkamp et al., 2008) with $Pbx1^{MN\Delta}$ and *Pbx3* heterozygote alleles (Figure 1E). The phenotypes of *Pbx1 flox/flox*;*Pbx3−/flox*;*Olig2*::Cre^{+} embryos were indistinguishable from that of $Pbx1^{MN\Delta}$;$Pbx3^{-/-}$ embryos at E12.5 (data not shown).

We assessed how loss of individual and multiple *Pbx* genes affects core features of MN identity and early rostrocaudal

(G) Summary shows Hox expression boundaries in MNs at brachial and thoracic levels.
(H) Hoxc6 and Hoxc9 boundaries are maintained in $Pbx^{MN\Delta}$ mutants, but Hoxc9 levels are reduced in PGC neurons.
(I) Hoxa5 and Hoxc8 boundaries are maintained in $Pbx^{MN\Delta}$ mutants.
(J and K) Misexpression of (J) Hoxc9 or a (K) Hoxc9-Pbx interaction mutant (Hoxc9IM) at brachial levels represses *Hoxc6*.
(L and M) Misexpression of (L) Hoxc6 or a (M) Hoxc6IM at thoracic levels represses *Hoxc9*.
See also Figure S1.

patterning. In $Pbx1^{MN\Delta}$, *Pbx3*, and $Pbx^{MN\Delta}$ embryos, markers for MN neurotransmitter synthesis, including choline acetyltransferase (Chat) and vesicular choline acetyltransferase transporter (Vacht), were present at E12.5, indicating *Pbx* genes are not required for generating MNs as a class (Figures 1F and S1E; data not shown). In addition, the MN progenitor determinants Olig2 and Nkx6.1 and the early postmitotic markers Isl1/2, Hb9, and Lhx3 were grossly unaltered in *Pbx* mutants (Figures 1D, 1E, and S1F). At thoracic levels, the total number of MNs was similar between control and $Pbx^{MN\Delta}$ mutants, although there was an ~30% reduction in MNs at limb levels, similar to the loss observed in *Foxp1* mutants (Figure 4I) (Dasen et al., 2008; Rousso et al., 2008). In $Pbx1^{MN\Delta}$ mutants, we also observed an expansion of the Pbx3 expression domain at caudal brachial levels (Figure S1G), although no changes in *Pbx2* and *Pbx4* expression were observed in any of the *Pbx* mutant alleles we analyzed (data not shown).

In the hindbrain, *Pbx* function has been implicated in positive autoregulatory interactions that maintain expression of *Hox* genes in specific rhombomeres (Tümpel et al., 2009). At spinal levels a major determinant of *Hox* gene expression is cross-repressive interactions between Hox proteins and *Hox* genes (Philippidou and Dasen, 2013). We therefore investigated a possible function of *Pbx* genes in controlling the pattern of *Hox* expression within the spinal cord. In $Pbx^{MN\Delta}$ mutants, the rostrocaudal boundaries between Hoxc6/Hoxc9 (brachial/thoracic boundary) and Hoxa5/Hoxc8 (rostral brachial/caudal brachial boundary) were preserved (Figures 1G–1I and S1I–S1K). In thoracic segments, Hoxc9 protein levels were reduced in MNs of $Pbx^{MN\Delta}$ mice at E12.5, while the overall patterns of Hoxa5, Hoxc6, and Hoxc8 were similar to controls (Figures 1H, 1I, and S1I–S1K). These observations indicate that Pbx proteins contribute to sustaining the levels of certain Hox proteins but are dispensable for cross-repressive interactions in spinal MNs.

To further assess whether Hox cross-repressive interactions can occur independently of Pbx function, we determined the effects of misexpressing Hox mutant derivatives in which the canonical Pbx interaction motifs have been mutated. We generated mutations within motifs N-terminal to the homeodomain, which are necessary for high-affinity interactions with Pbx proteins on DNA. Misexpression of a Hoxc9 derivative with a mutated Pbx interaction motif (Hoxc9IM NW→AA) in chick neural tube was able to repress *Hoxc6*, *Hoxa5*, and LMC specification at brachial levels (Figures 1J, 1K, and S1L). However, unlike wild-type Hoxc9, this mutation failed to induce PGC neurons at brachial levels (Figure S1L). As previously reported, Hoxc6IM repressed *Hoxc9* at thoracic levels (Figures 1L and 1M). Hoxc6IM can induce an LMC fate at thoracic levels (Lacombe et al., 2013), likely as a consequence of *Hoxc9* attenuation. Although we cannot rule out the possibility that Hox proteins interact with Pbx proteins through additional domains (Merabet and Mann, 2016), these results indicate that *Pbx* genes are not required for establishing the overall rostrocaudal pattern of *Hox* expression in MNs.

Pbx Genes Are Essential for the Differentiation of Hox-Dependent MN Subtypes

We next examined the function of *Pbx* genes in the diversification of segmentally restricted MN subtypes. At limb levels, LMC neurons are defined by expression of the transcription factor *Foxp1* and the retinoic acid (RA) synthetic enzyme *Raldh2* (Dasen et al., 2008). In *Pbx3* mutants Foxp1 and Raldh2, expression was unaltered at brachial levels (Figure S2A). In $Pbx1^{MN\Delta}$ embryos, we observed a marked reduction in the number of brachial $Foxp1^+$, $Raldh2^+$ neurons (Figures S2D and S2E), although the penetrance of this phenotype was apparently offset by the upregulation of Pbx3 within this region (Figure S1G). Analysis of mice lacking both *Pbx1* and *Pbx3* revealed a dramatic reduction in Foxp1 and Raldh2 expression (Figures 2A and 2B). Raldh2-dependent RA synthesis in LMC neurons provides a feedback signal that promotes the proliferation of MN progenitors (Sockanathan and Jessell, 1998), and the loss of this signal likely accounts for the decrease in brachial MNs in *Pbx* mutants. These results indicate *Pbx* genes are essential to establish the identity and normal number of LMC neurons.

Hox genes are critical for the further differentiation of LMC neurons into divisional and pool subtypes, which determine how motor axons select muscle targets in the limb (Dasen et al., 2005). Expression of Lhx1 in the lateral division of the LMC defines MNs that project to the dorsal limb compartment (Kania, 2014), and this population of $Lhx1^+$, $Foxp1^+$ neurons was depleted in $Pbx^{MN\Delta}$ mutants (Figures 2C and 2D). Within the LMC, neurons targeting individual limb muscles segregate into MN pools, some of which can be defined by the expression of specific transcription factors. In $Pbx^{MN\Delta}$ mice, we observed a loss of MN pools marked by Scip, Nkx6.1, and Nkx6.2 expression (Figures 2I–2K). Expression of the pool marker Pea3 was preserved in $Pbx^{MN\Delta}$ mutants (Figure 2L), consistent with studies suggesting Pbx-independent regulation of its expression (Catela et al., 2016; Lacombe et al., 2013) and reliance on peripheral signaling to control its induction (Figures S2F–S2H) (Haase et al., 2002). *Pbx* genes are therefore essential for the appearance of multiple molecular features of LMC subtypes.

At thoracic levels, *Hox* genes are necessary for the differentiation of PGC neurons that innervate the sympathetic chain ganglia (scgs). PGC neurons express neuronal nitric oxide synthase (nNos), phospho (p)Smad1/5/8, Isl1, low levels of Foxp1, and settle dorsolaterally (Dasen et al., 2008). In $Pbx^{MN\Delta}$ mutants, nNos and pSmad expression is lost from MNs and $Isl1^+$ MNs fail to migrate to a dorsolateral position (Figures 2E–2H). Interestingly, the differentiation of PGC neurons also relied on the net level of *Pbx* expression in MNs, as $Pbx1^{MN\Delta}$;$Pbx3^{+/-}$ mutants (which retain a single copy of *Pbx3*) also displayed dramatically reduced numbers of PGC neurons (Figures S2B and S2C). The dose-dependent phenotypes of Pbx mutant alleles likely reflect differences in the level and pattern of Pbx1 and Pbx3 within specific MN subtypes (Figures S1A–S1D).

In addition to these well-characterized Hox-dependent MN populations, other segmentally restricted subtypes were affected in *Pbx* mutants. At rostral cervical levels, two non-LMC ($Foxp1^-$) populations of MNs can be defined by the expression of the transcription factors Sox5 and Scip (Philippidou et al., 2012). Sox5 is expressed by a laterally positioned $Lhx3^+$, $Hb9^+$, $Isl1^+$ MN pool, and this population was lost in $Pbx^{MN\Delta}$ mice (Figure 2M). MNs within the phrenic motor column (PMC) rely on the activities of

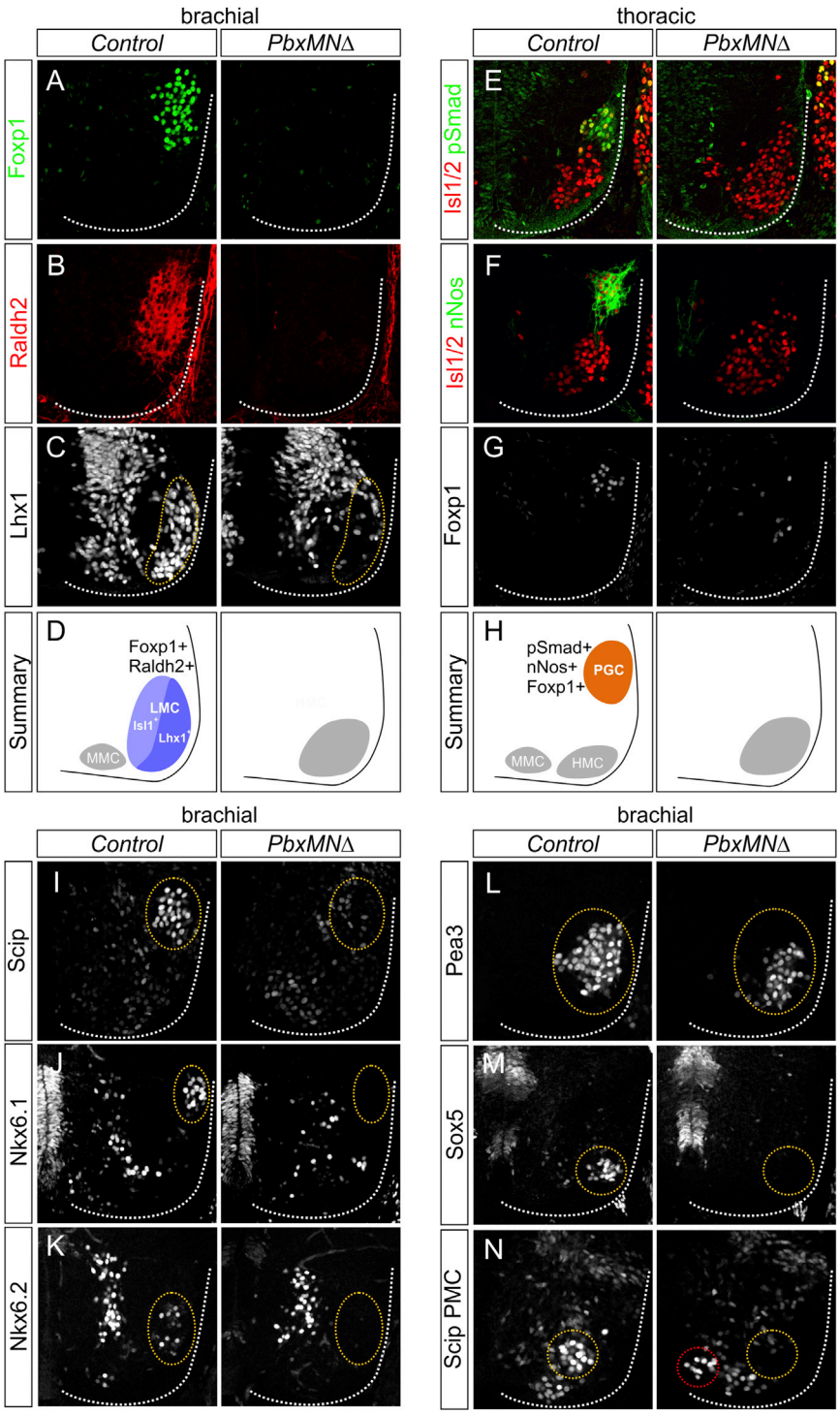

Figure 2. *Pbx* Genes Are Essential for MN Columnar, Divisional, and Pool Specification

(A and B) Expression of (A) Foxp1 and (B) Raldh2 is reduced in $Pbx^{MN\Delta}$ mutants at E12.5.

(C) Expression of Lhx1 within the lateral division of the LMC is depleted at brachial levels in $Pbx^{MN\Delta}$ mice.

(D) Summary shows LMC neuron organization at brachial levels in control and $Pbx^{MN\Delta}$ mice.

(E–G) At thoracic levels, there is a loss of (E) pSmad, (F) nNos, and (G) Foxp1 expression in $Pbx^{MN\Delta}$ mutants.

(H) Summary shows MN organization at thoracic levels in control and $Pbx^{MN\Delta}$ mice.

(I) Loss of Scip expression from median and ulnar MN pools in $Pbx^{MN\Delta}$ mice is shown.

(J and K) Loss of (J) Nkx6.1 and (K) Nkx6.2 expression from rostral brachial pools in $Pbx^{MN\Delta}$ mutants.

(L) Expression of Pea3 is detected in $Pbx^{MN\Delta}$ mice but is mispositioned ventromedially.

(M) Loss of the non-LMC $Sox5^{+}$ pool in $Pbx^{MN\Delta}$ mice is shown.

(N) Expression of Scip in phrenic MNs is reduced and mislocalized (red circle) in $Pbx^{MN\Delta}$ mice. In (I)–(N), circled areas discriminate MNs that express indicated factors from other spinal populations. In $Pbx^{MN\Delta}$ mice, circled areas represent the positions where these pools would be present normally.

See also Figure S2.

Hox5 genes and coexpress Scip and Isl1. In $Pbx^{MN\Delta}$ embryos, this population is reduced, disorganized, and shifted to a more medial position (Figure 2N). Interestingly, both $Scip^{+}$ PMC and $Sox5^{+}$, $Lhx3^{+}$ MNs are retained in *Foxp1* mutants (Dasen et al., 2008; Rousso et al., 2008), indicating that loss of *Pbx* genes affects most segmentally restricted MN subtypes.

Peripheral Innervation Defects in *Pbx* Mutants

Because molecular signatures of Hox-dependent MN subtypes are lost in $Pbx^{MN\Delta}$ mice, we next determined the impact of *Pbx* mutation on the trajectory and target selectivity of motor axons. We bred $Pbx^{MN\Delta}$ mutant mice to *Hb9*::*GFP* mice, in which all motor axons are GFP labeled, and analyzed the overall pattern of peripheral innervation. Projections into the limb were detectable in $Pbx^{MN\Delta}$;*Hb9*::*GFP* mutants at E12.0, but at subsequent time points the distal nerve branches were thinner and specific target regions lacked innervation (Figures 3A and 3B). Nerve branches to muscles in the proximal forelimb were missing or stunted in $Pbx^{MN\Delta}$ mutants, including a severe reduction in the density of projections along the radial nerve (Figures 3A and 3B). $Pbx^{MN\Delta}$;*Hb9*::*GFP* mice also displayed pronounced innervation defects within the hindlimb. The most striking defect was observed along the tibialis anteroir nerve, which was completely absent in $Pbx^{MN\Delta}$ mice at E13.5 (Figures 3C and 3D).

At thoracic levels, MNs within the PGC pursue a ventromedial trajectory toward scgs, and subsequently they send collateral

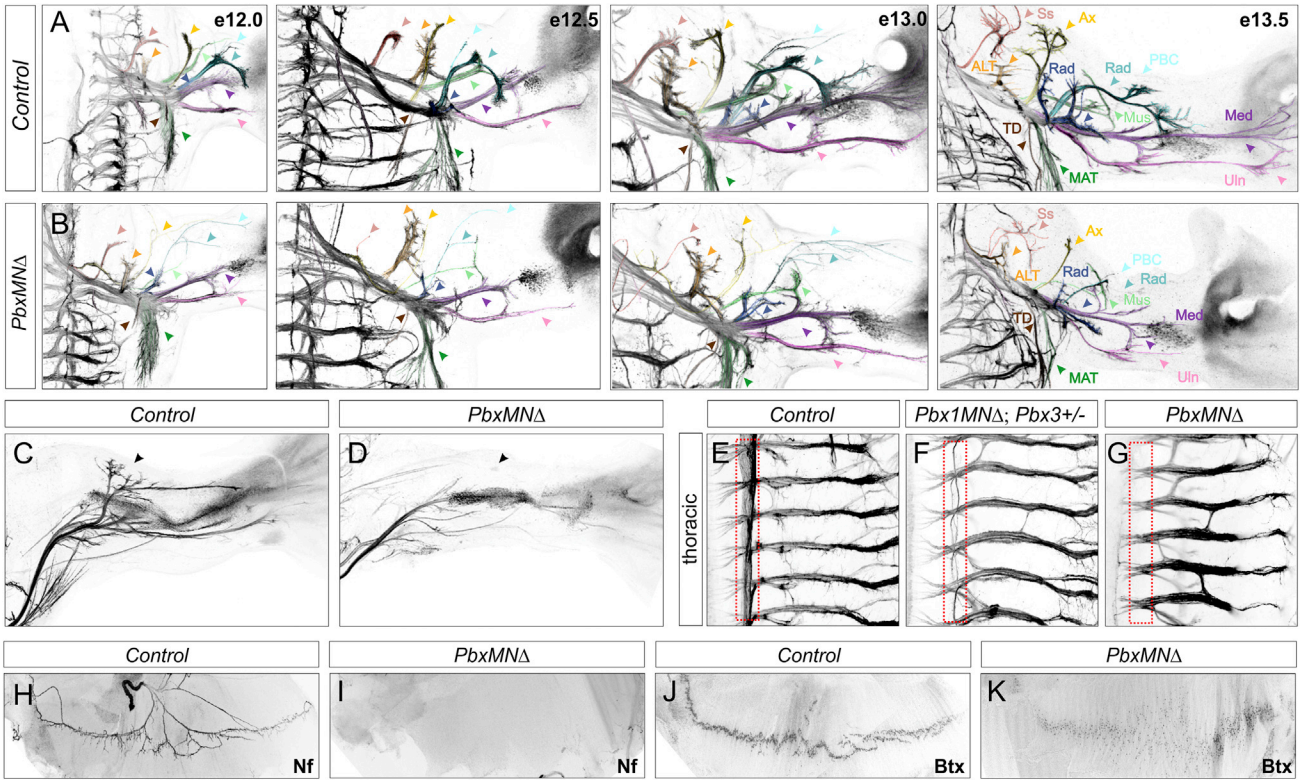

Figure 3. Motor Axon Projections in *Pbx*$^{MN\Delta}$ Mice

(A and B) Dorsal view of forelimb innervation in (A) control and (B) *Pbx*$^{MN\Delta}$ mice between E12.0 and E13.5. *Pbx*$^{MN\Delta}$ mice have thinner axons and display defects in axonal branching and nerve trajectories. Suprascapular nerve (Ss), red; anterior lateral thoracic nerve (ALT), orange; axillary nerve (Ax), yellow; musculocutaneous nerve (Mus), neon green; radial nerve (Rad), blue; posterior brachial cutaneous nerve (PBC), aqua; radial/musculospiral nerve (Rad), dark blue; median nerve (Med), dark purple; ulnar nerve (Uln), light purple; thoracodorsal nerve to lattismus dorsi (TD), brown; medial anterior thoracic nerve to the cutaneous maximus (MAT), dark green.

(C and D) In *Pbx*$^{MN\Delta}$;*Hb9*::*GFP* mice, the dorsal tibialis anterior nerve fails to form in the hindlimb.

(E–G) Motor axon projections at thoracic levels showing loss of scg innervation (outlined in red). Mice retaining one allele of *Pbx3* also display projection defects. Projections along the intercostal nerves are retained in *Pbx* mutants, although some aberrant branching is observed.

(H and I) Diaphragm innervation defects in *Pbx*$^{MN\Delta}$ mutants at E16.5. Motor axons are labeled using neurofilament (Nf) staining. In *Pbx*$^{MN\Delta}$ mice, phrenic axons fail to innervate the diaphragm.

(J and K) Staining with α-bungarotoxin (Bgt) shows acetylcholine receptor (AChR) clustering in (J) control animals and the absence of concentrated clusters in (K) *Pbx* $^{MN\Delta}$ mice.

See also Figure S3.

projections that extend along the rostrocaudal axis. In whole-mount staining of control *Hb9*::*GFP* mice, these projections are visible as a medial GFP^{+} band that extends parallel to the spinal cord (Figures 3E, S3C, and S3D). In *Pbx*$^{MN\Delta}$ mutants, projections toward and between scgs were dramatically reduced (Figures 3G, S3A, S3B, S3G, and S3H). Similarly, in *Pbx1* conditional mutants retaining one copy of *Pbx3*, there was a pronounced decrease in scg innervation (Figures 3F, S3E, and S3F). In contrast, motor nerves projecting to axial and hypaxial muscles (which derive from MMC and thoracic HMC neurons, respectively) were preserved in *Pbx*$^{MN\Delta}$ mutants (Figure 3G).

One of the most severely affected nerve branches in *Pbx* mutants derives from phrenic MNs that extend to the diaphragm muscle. At E12.5 the phrenic nerve was visible in *Pbx*$^{MN\Delta}$;*Hb9*::*GFP* mutants, but it was dramatically thinner and shorter than in control littermates (Figures S3I and S3J). By E16.5 there was a severe loss of synapses at the diaphragm, with the majority of muscle fibers lacking innervation and post-synaptic acetyl choline receptor clusters (Figures 3H–3K). The severe defects in diaphragm innervation likely account for the perinatal lethality of *Pbx*$^{MN\Delta}$ mutants.

Motor Columns Are Disorganized in *Pbx* Mutants

What are the fates of the remaining MN populations after deletion of *Pbx* genes? In mice mutant for the Hox accessory factor *Foxp1*, LMC and PGC neurons acquire the identity of thoracic HMC neurons, while axially projecting MMC neurons are unaffected (Dasen et al., 2008). In *Pbx* mutants, the number of Lhx3^{+}, Hb9^{+} MMC neurons was not significantly altered at brachial and thoracic levels (Figures 4A–4I). The remaining populations consisted predominantly of MNs with an HMC-like molecular profile (Hb9^{+};Isl1/2^{+}) as well a smaller group that expressed Isl1/2 alone (Figures 4I and S4A–S4D). These results indicate that, in the absence of *Pbx* function, the

remaining MNs display molecular features of MMC and HMC subtypes.

Analysis of the distribution of MNs in *Pbx* mutants revealed a striking disorganization in their settling position. In $Pbx^{MN\Delta}$ mice, Lhx3$^+$, Hb9$^+$ (MMC-like); Hb9$^+$, Isl1/2$^+$ (HMC-like); and Isl1/2$^+$ MNs were intermixed at E12.5 (Figures 4A–4H). This phenotype was observed at all rostrocaudal levels of the spinal cord and was particularly prominent at thoracic levels. Comparison of serial sections in *Pbx* mutants revealed no positional preference of MMC and non-MMC neurons, indicating they are stochastically positioned within the ventral spinal cord (Figures 4A–4H). In contrast, the organization and specification of ventral interneurons was not affected in $Pbx^{MN\Delta}$ mice (Figure S4G). To quantify the degree of MN intermixing in *Pbx* mutants, we calculated a columnar mixing index (Cmi) for thoracic MMC and HMC neurons in control and mutant mice at E12.5 (Demireva et al., 2011). This allowed us to determine the extent to which MMC neurons invade the confines of the HMC and HMC invasion into the MMC. In control thoracic sections, Cmi values for MMC→HMC and HMC→MMC averaged 0.14 and 0.15, respectively. In *Pbx* mutants, this value increased to 0.90 for MMC→HMC and 0.85 for HMC→MMC (Figure 4J).

Because the transcription factors used to discriminate columnar identities (Lhx3, Hb9, and Isl1/2) are expressed by the precursors to all MN subtypes, we considered the possibility that the observed intermixing is not due to migratory or clustering defects, but rather a failure of MNs to fully differentiate in $Pbx^{MN\Delta}$ mice. If, however, the remaining columnar subtypes are properly differentiated, they would be predicted to target muscles appropriate for their molecular identity. Because loss of an LMC identity leads to a random targeting of limb muscles by MNs (Dasen et al., 2008; Rousso et al., 2008), we assessed the targeting of MMC and HMC neurons at thoracic levels, where these two populations are present normally. We injected tracers into the intercostal nerves (targets of HMC neurons) or axial muscles (targets of MMC neurons) in control and $Pbx^{MN\Delta}$ mutants at E12.5, and we monitored the transcriptional profile of retrogradely labeled MNs. After tracer injection into the intercostal nerves of $Pbx^{MN\Delta}$ mutants, labeled MNs exhibited an HMC profile (Isl1/2$^+$, Hb9$^+$) and lacked Lhx3 (Figure 4K). After injection into axial muscles, labeled MNs exhibited an MMC profile (Lhx3$^+$, Hb9$^+$, Isl1/2^{low}) (Figure 4K). In agreement with the analysis of MMC and HMC molecular profiles, retrogradely labeled neurons lacked any clear columnar organization. These results indicate that, despite their altered position, the remaining thoracic MMC and HMC neurons in $Pbx^{MN\Delta}$ mice differentiate and select appropriate muscle targets. In contrast, retrograde labeling from the forelimb ulnar nerve labeled MNs with an HMC-like profile (Isl1$^+$, Lhx3$^-$) that were dispersed within the spinal cord (Figure S4H), similar to *Foxp1* mutants (Dasen et al., 2008).

Several lines of evidence indicate that the intermixing of HMC and MMC neurons reflects a unique function of *Pbx* genes during MN differentiation. Analysis of *Foxp1* mutants revealed a loss of Hox-dependent subtypes at limb and thoracic levels, with the remaining MNs consisting predominantly of HMC and MMC neurons (Dasen et al., 2008; Rousso et al., 2008). Despite the similarity in the loss of MN identities in *Foxp1* and *Pbx* mutants, in the absence of *Foxp1* the remaining HMC and MMC neurons were clustered and well segregated (Figures 4L and S4E). In mice lacking the *HoxA* and *HoxC* gene clusters, Hox-dependent MN subtypes are similarly lost at brachial and thoracic levels (Jung et al., 2014). The *HoxA* and *HoxC* clusters encode the majority of Hox proteins expressed at these levels and, therefore, approximate a Hox-less ground state. In combined *HoxA* and *HoxC* mutants, the clustering and segregation of the remaining subtypes (MMC, HMC, and Isl1/2$^+$ MNs) was unaffected (Figures 4M and S4F) (Jung et al., 2014). Calculation of Cmis in *Foxp1* and *HoxA/C* mutants revealed no increase in thoracic MMC/HMC intermixing relative to Cmi values of control littermates (Figure 4J). These observations suggest a unique, and possibly Hox-independent, function for Pbx proteins in the organization of columnar subtypes projecting to epaxial and hypaxial muscles (Figure 4N).

Identification of Genes Selectively Depleted in *Pbx* Mutants

The intermixing of the remaining MMC and non-MMC neurons in $Pbx^{MN\Delta}$ mice prompted us to consider whether *Pbx* genes might selectively regulate target effectors present in these populations. To explore this possibility, we analyzed a panel of genes demonstrated to be downstream of MN fate determinants. We reasoned that genes that facilitate the segregation and clustering of MMC and non-MMC populations would be specifically lost in *Pbx* mutants, but they would be maintained under conditions where columnar segregation is preserved, such as in *Foxp1* mutants. We screened over two dozen genes, including members of the *cadherin* and *ephrin/Eph* gene families, which have been implicated in neuronal migration and clustering within the hindbrain and spinal cord (Kania, 2014). This analysis identified a number of motor pool-restricted genes that are diminished in $Pbx^{MN\Delta}$ mice, although the majority of these genes also was downregulated in *Foxp1* mutants (Figures S5A–S5E; data not shown).

These results encouraged us to initiate an unbiased screen to identify genes selectively lost in $Pbx^{MN\Delta}$ mice. We compared gene expression profiles in MNs isolated from control and $Pbx^{MN\Delta}$ embryos at E12.5. We purified MNs from $Pbx^{MN\Delta}$;*Hb9*::*GFP* and control *Hb9*::*GFP* embryos by fluorescence-activated cell sorting (FACS) (Figure 5A). Due to the distinct molecular profiles of MNs generated at brachial and thoracic levels, we independently profiled both populations. We extracted RNA from MNs purified from nine $Pbx^{MN\Delta}$;*Hb9*::*GFP* and nine *Hb9*::*GFP* embryos at brachial and thoracic levels, pooled three RNA samples of each genotype, and prepared 12 bar-coded libraries. We then performed expression profiling by RNA sequencing (RNA-seq). The samples were mixed into two pools and run on two 50-nt paired-end read rapid-run flow cell lanes with the Illumina HiSeq 2500 sequencer.

To evaluate the quality of this screen, we examined the expression of genes known to be differentially expressed between brachial and thoracic levels. Comparison of expression profiles between purified control samples yielded known cervical/brachial (*Aldh1a2/Raldh2*, *Etv4/Pea3*, *Runx1*, *Lypd1/Lynx2*, and *Hoxc6*) and thoracic level- (*nNos*, *Etv1/Er81*, and *Hoxc9*) restricted MN determinants (Figure 5B; Table S1). Read counts of *HoxC* cluster genes were similar between control and $Pbx^{MN\Delta}$

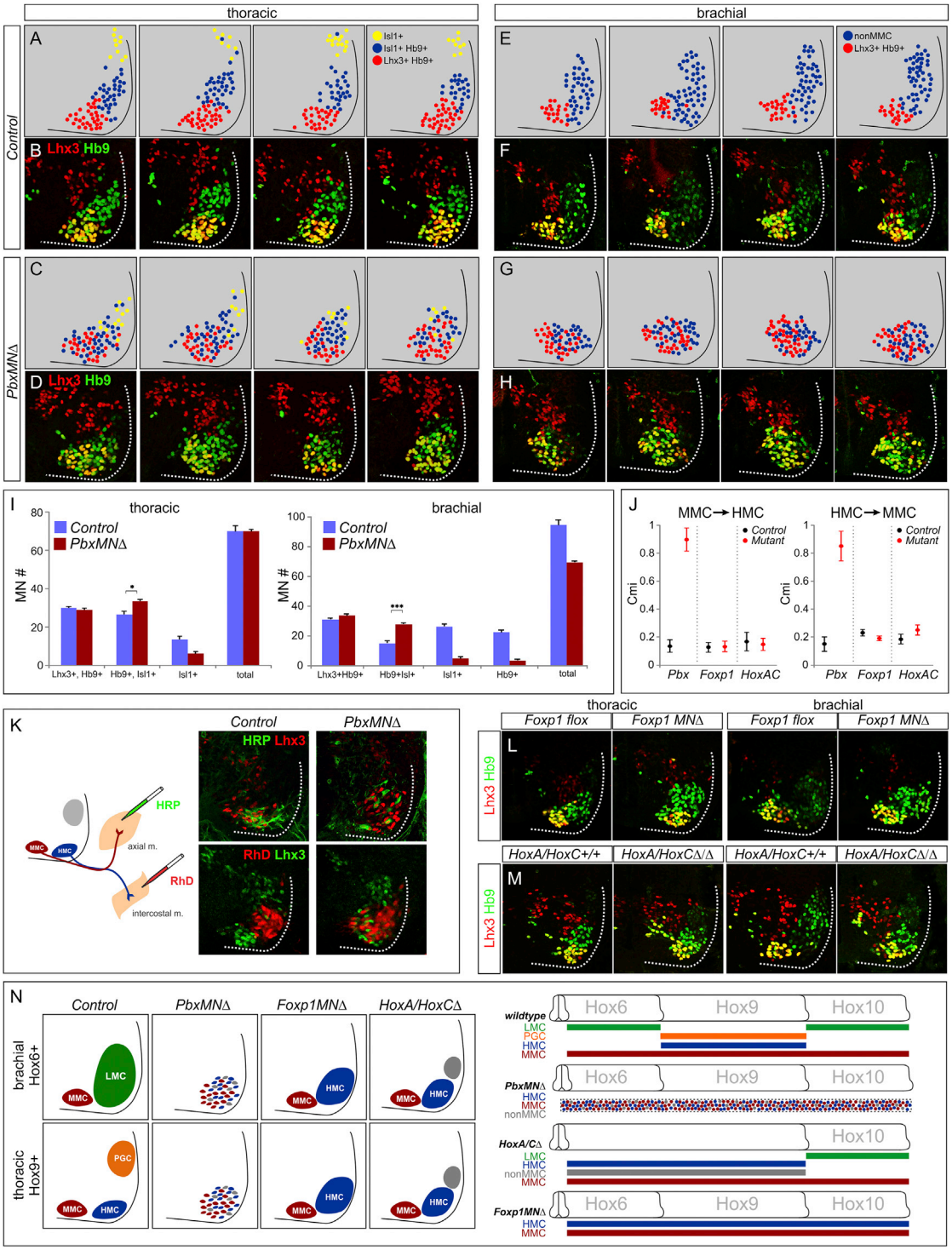

Figure 4. MN Columnar Disorganization in *Pbx*$^{MN\Delta}$ Mice

(A–D) Position of molecularly defined thoracic MN subtypes in (A and B) control and (C and D) *Pbx*$^{MN\Delta}$ mice at E12.5. Schematics represent serial thoracic sections of control and *Pbx* mutants indicating the position of MN subtypes defined by Lhx3, Hb9, and Isl1 expression. MMC neurons are Lhx3$^+$, Hb9$^+$; HMC neurons are Hb9$^+$, Isl1$^+$, Lhx3$^-$; and PGC neurons are Isl1$^+$.

(E–H) Position of MN subtypes at brachial levels. Non-MMC neurons are defined as MNs that are Lhx3$^-$ and express Hb9 and/or Isl1. Brachial sections shown are from segments C6–C8.

(legend continued on next page)

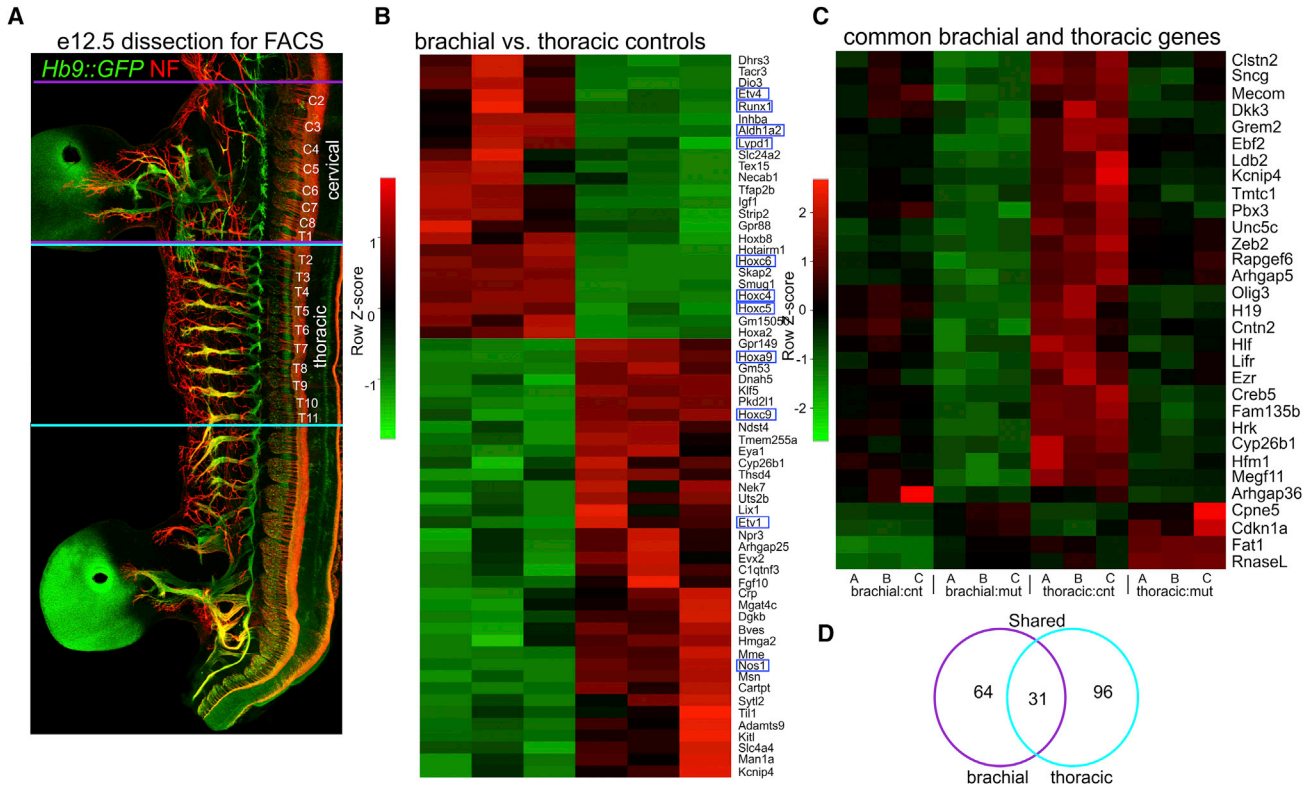

Figure 5. Identification of Pbx Gene Targets in MNs

(A) Whole-mount staining of *Hb9*::*GFP* mouse at E12.5 showing dorsal root ganglia (DRGs) and spinal segmental levels used for gene profiling. Nf staining highlights the segments isolated for FACS. Brachial MNs were isolated from cervical (C) level C2 to thoracic (T) level T1 and thoracic MNs were isolated from T2 to T11.

(B) Heatmap showing comparison of gene expression differences between brachial and thoracic MNs in controls. Known differentially expressed genes are outlined in blue.

(C) Heatmap showing expression differences between control and $Pbx^{MN\Delta}$ mutants. Heatmap lists genes that are common to both brachial and thoracic samples and that are differentially expressed with a p adjusted < 0.05 cutoff. Heatmaps for each of the three pools are shown and are labeled A, B, and C.

(D) Venn diagram shows differentially expressed genes shared between brachial and thoracic levels.

See also Figure S5.

mice at both brachial and thoracic levels (Figure S6E), reinforcing the conclusion that the *Hox* patterns are grossly preserved in $Pbx^{MN\Delta}$ mice.

Because the loss of *Pbx* genes affects MN organization at all rostrocaudal levels, we focused on genes whose profiles were altered at both brachial and thoracic levels. Comparison of gene profiles within brachial and thoracic MNs identified 31 transcripts (27 downregulated and 4 upregulated genes) that were common to both populations and differentially expressed between control and *Pbx*-mutant mice (Figures 5C, 5D, and S6A–S6D; Tables S2 and S3). To validate these targets, we used in situ hybridization to compare expression patterns of candidates between control and $Pbx^{MN\Delta}$ mice at E12.5. Analysis of the 27 downregulated candidates identified 13 that were expressed by MNs in control animals (Figures 6A–6M; data not shown). Each of these genes was undetectable or markedly downregulated in MNs of $Pbx^{MN\Delta}$ mice, confirming them as Pbx targets (Figures 6A–6M). Novel genes that were upregulated in $Pbx^{MN\Delta}$ mice and validated by in situ hybridization included *Cpne5* and *Cdkn1a* (Figures 6N and 6O). In control embryos,

(I) Quantification of MN subtypes in control and *Pbx* mutants at brachial and thoracic levels. Molecular codes for columnar subtypes are indicated. MN counts show average of indicated subtype on one side of spinal cord ± SEM. *p < 0.05 and ***p < 0.001.

(J) Quantification of columnar mixing indices (Cmis) for the indicated mutant at thoracic levels. Data are shown as mean Cmi ± SEM, averaged from n > 4 sections and from n > 3 animals of the indicated genotype.

(K) Retrograde labeling of HMC and MMC neurons in control and $Pbx^{MN\Delta}$ mice at E12.5. MMC neurons were labeled by injection of horseradish peroxidase (HRP) into axial muscles, and HMC neurons were labeled by injection of intercostal nerves with rhodamine dextran (RhD).

(L and M) Comparison of MN organization at thoracic levels in control, $Pbx^{MN\Delta}$, *Foxp1*, and *HoxA/C* mutants. In *Foxp1* and *HoxA/C* mutants, MMC neurons are organized and segregated from non-MMC neurons.

(N) Summary shows defects in MN specification and positioning in *Pbx*, *Foxp1*, and *Hox* cluster mutants.

See also Figure S4.

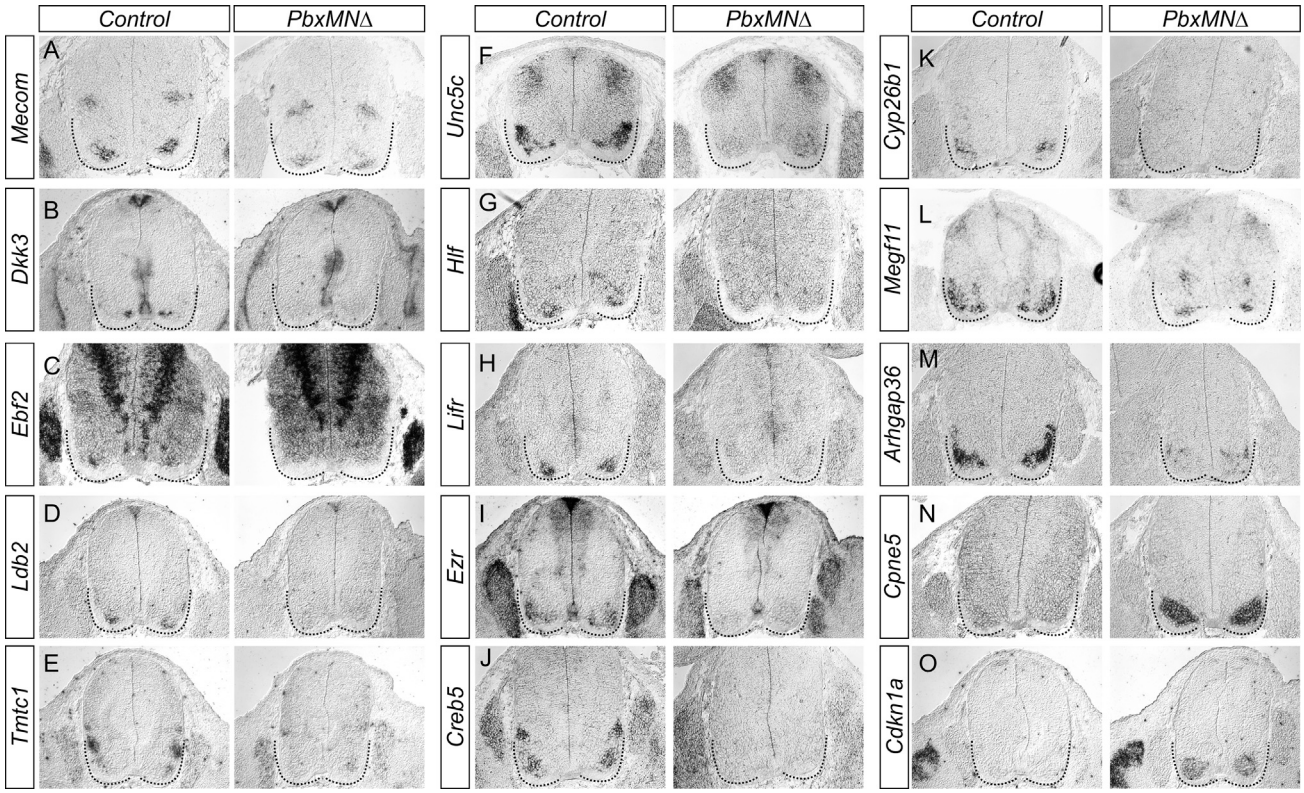

Figure 6. Characterization of Pbx Target Gene Expression in MNs

(A–O) Analysis of genes common to brachial and thoracic levels that are differentially expressed between control and $Pbx^{MN\Delta}$ mice. Panels show in situ hybridization of indicated genes in spinal cord sections of E12.5 mice. All sections are brachial except (J) and (K), which are thoracic. Sections are derived from embryos that are *Pbx1 flox/flox*;*Pbx3−/flox*;*Olig2*::Cre^{+}.

(A) *Mecom* is downregulated in ventromedial neurons but preserved in dorsal interneurons.

(B–K) Expression of (B) *Dkk3*, (C) *Ebf2*, (D) *Ldb2*, (E) *Tmtc1*, (F) *Unc5c*, (G) *Hlf*, (H) *Lifr*, (I) *Ezr*, (J) *Creb5*, and (K) *Cyp26b1* is markedly decreased in MNs of *Pbx* mutants.

(L) *Megf11* is downregulated in LMC neurons but maintained in a subset of ventromedial MNs.

(M) *Arhgap36* expression is markedly reduced in $Pbx^{MN\Delta}$ mice.

(N and O) As shown, (N) *Cpne5* and (O) *Cdkn1a* are upregulated in *Pbx* mutants.

See also Figure S6.

Cpne5 was weakly expressed by MNs with elevated expression in MMC neurons (Figure 6N). In $Pbx^{MN\Delta}$ mice, *Cpne5* expression was markedly upregulated in all remaining MNs (Figure 6N). Additional genes from this list were either not detected by in situ hybridization or expressed by non-MN populations (data not shown).

Among the confirmed downregulated genes in *Pbx* mutants were a number that were restricted to ventral spinal populations. Included in this group were the cell surface proteins *Lifr* and *Megf11*, the secreted protein *Dkk3*, the intracellular protein *Ezr*, and the transcription regulators *Mecom*, *Ebf2*, *Ldb2*, *Hlf*, and *Creb5* (Figures 6A–6D, 6G–6J, and 6L). Expression of *Lbd2*, *Hlf*, *Lifr*, and *Creb5* was not detectable in the spinal cords of $Pbx^{MN\Delta}$ mice at E12.5, while expression of *Mecom*, *Dkk3*, *Ezr*, and *Megf11* was selectively lost from subsets of MNs (Figure 6). *Mecom* was expressed in ventromedial MN populations as well as a dorsal interneuron population at all rostrocaudal levels. In $Pbx^{MN\Delta}$ mutants, expression of *Mecom* was markedly diminished in MNs, while its pattern in dorsal interneurons was unaffected (Figure 6A). Expression of *Mecom*, *Dkk3*, *Ebf2*, *Ldb2*, *Hlf*, *Lifr*, and *Cyp26b1* also was maintained in *Foxp1* mutants, while *Cpne5* and *Cdkn1a* were not upregulated (Figures S5F–S5T), suggesting regulation of these targets independent of the Hox/Foxp1-dependent programs acting in non-MMC neurons.

Mecom Defines a Pbx-Dependent Population of MNs Targeting Axial Muscle

The identification of MN subtype-restricted genes that are selectively downregulated in *Pbx* mutants enabled us to further assess a potential Hox-independent function of Pbx proteins during MN specification. Due to its restricted expression in ventromedial MN populations, *Mecom* was chosen for further analysis. We characterized the pattern of *Mecom* expression relative to MN determinants between E9.5 and E12.5. Mecom protein was first detected at E9.5 as the first brachial postmitotic MNs appear, and subsequently it was maintained in a subset of medial MNs (Figures 7A, 7B, and S7A). At E12.5 Mecom colocalized with markers for MMC identity at all rostrocaudal levels of

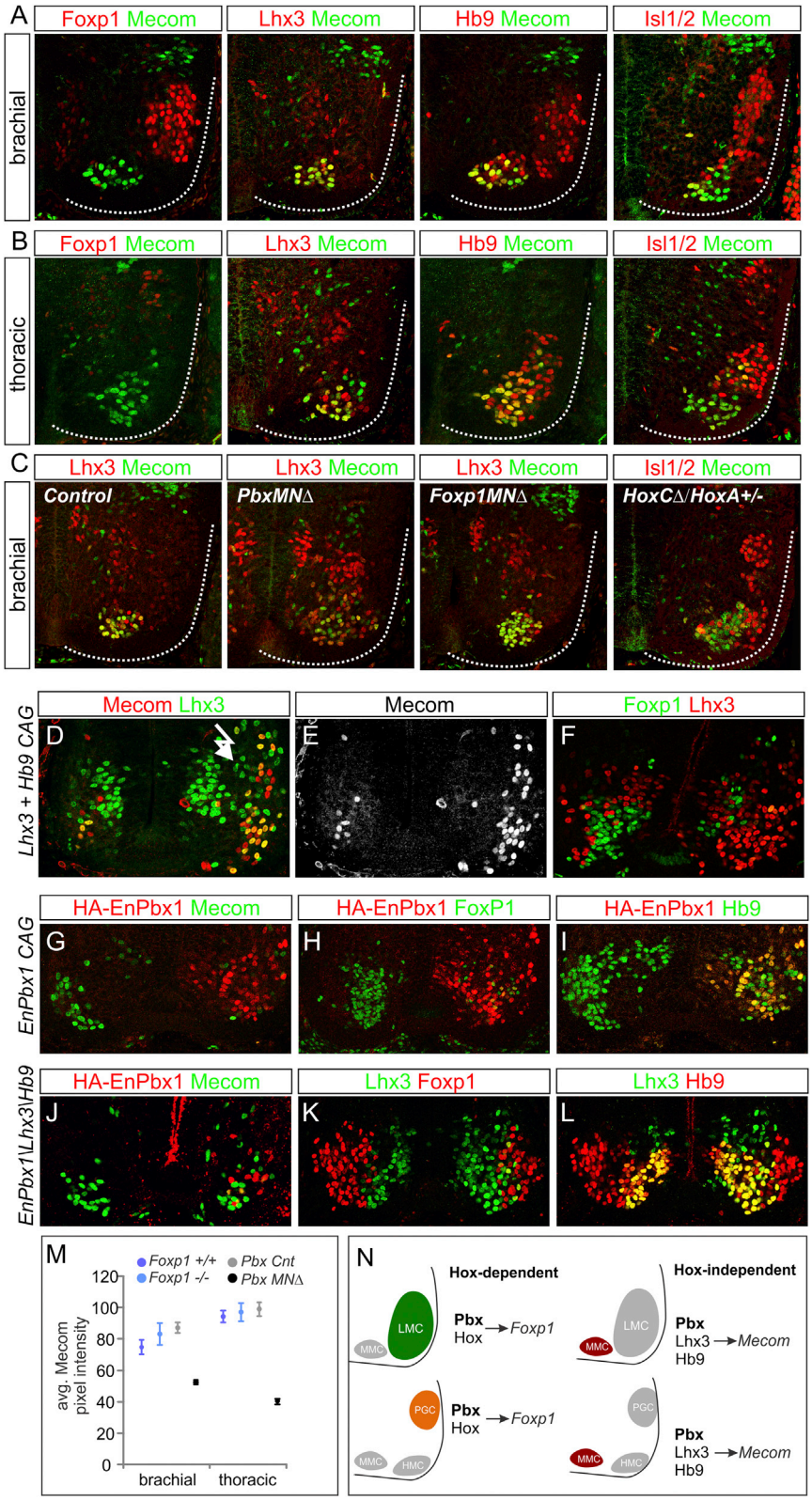

Figure 7. Hox-Independent Regulation of *Mecom* by Pbx Proteins and Lhx3

(A) Mecom protein expression at brachial levels at E12.5. Mecom is detected in Lhx3$^+$, Hb9$^+$ MMC neurons, but it is excluded from Foxp1$^+$ LMC neurons.

(B) Mecom expression at thoracic levels. Mecom is detected in MMC neurons, a subset of Lhx3$^-$, Hb9$^+$ MNs, but it is excluded from Foxp1$^+$ PGC neurons.

(C) Analysis of Mecom expression in *Pbx*, *Foxp1*, and *HoxC* mutants. Mecom is reduced in MMC neurons of *Pbx* $^{MN\Delta}$ mice, but it is unaffected in *Foxp1*$^{MN\Delta}$ and *HoxC* mutants.

(D and E) Chick electroporations at thoracic levels showing Mecom expression is induced after *Lhx3* and *Hb9* misexpression.

(F) Lhx3/Hb9 also represses *Foxp1* expression.

(G–I) Expression of *EnPbx1* represses Mecom and Foxp1 in MNs.

(J–L) Coexpression of *EnPbx1*, *Lhx3*, and *Hb9* fails to generate ectopic Mecom$^+$ MNs.

(M) Quantification of Mecom levels in *Pbx* and *Foxp1* mutants. Data are shown as average pixel intensities of Mecom immunofluorescence ± SEM.

(N) Summary MN columnar specification by Pbx proteins. Pbx proteins act in Hox-dependent pathways to induce expression of columnar determinants, such as *Foxp1*. Pbx proteins also act in a Hox-independent manner to regulate expression of MMC-restricted genes, including *Mecom*.

See also Figure S7.

the spinal cord, but it was excluded from Foxp1$^+$ LMC and PGC neurons (Figures 7A and 7B). In addition, Mecom was absent from rostral brachial Sox5$^+$, Lhx3$^+$ MNs, but it was present in a small subset of thoracic Lhx3$^-$, Foxp1$^-$ MNs (Figures 7B and S7B). The MMC-restricted pattern of Mecom also was conserved in MNs of chick embryos (Figure S7C). Mecom therefore defines a novel postmitotic marker labeling MMC neurons projecting to dorsal axial muscles.

We next investigated the regulation of *Mecom* by Pbx proteins and other MN subtype determinants. In *Pbx*$^{MN\Delta}$ mutants, the level of Mecom protein expression was markedly reduced, with low levels detected in the remaining scattered Lhx3$^+$ MMC cells (Figures 7C and 7M). In contrast, the pattern of Mecom expression was unaffected in *Foxp1* and *HoxC* cluster mutants, and its restriction to MMC neurons was retained (Figure 7C). These observations provide additional in vivo evidence that Pbx proteins function independently of the Hox/Foxp1 program to regulate expression of MMC-restricted genes such as *Mecom*.

If *Mecom* is regulated by Pbx proteins independently of Hox function, its expression could reflect an output of an earlier MMC-specific differentiation program. We therefore tested if determinants of MMC identity can induce expression of *Mecom* in non-MMC neurons. Misexpression of the Hb9 transcription factor has been shown to impose an MN fate on interneurons, while expression of Lhx3 in all MNs directs an MMC fate (Sharma et al., 2000; William et al., 2003). Because expression of Lhx3 in non-MNs produces predominantly V2a interneurons, while expression of Hb9 generates MNs with either MMC or HMC-like properties (Dasen et al., 2008; Thaler et al., 2002), we coexpressed both factors to produce ectopic MMC neurons. We found that misexpresion of Lhx3 and Hb9 induced ectopic Mecom$^+$ MNs (Figures 7D, 7E, and S7D). Lhx3 and Hb9 coexpression also extinguished expression of *Foxp1*, a known target of Hox proteins in MNs (Figure 7F).

To test whether the supernumerary Mecom$^+$ MNs induced by Lhx3 and Hb9 require Pbx function, we expressed these factors in conjunction with a dominant-negative Engrailed-repressor fusion with Pbx1 (EnPbx1). Expression of EnPbx1 alone repressed Mecom and Foxp1, but not Hb9, consistent with Pbx1 activity being required for the differentiation of MMC and LMC neurons (Figures 7G–7I). In contrast, coexpression of Lhx3, Hb9, and EnPbx1 failed to generate Mecom$^+$ MMC neurons (Figures 7J–7L). Collectively, these results show that *Pbx* genes are essential for the normal expression of *Mecom* in MNs, and they act in concert with Lhx3 to determine its MMC-restricted pattern (Figure 7N). Pbx proteins, therefore, appear to act in parallel Hox-dependent and -independent programs to control the subtype differentiation and organization of MN subtypes.

DISCUSSION

The clustering of MNs into longitudinally arrayed columnar groups is a defining feature of topographical maps within tetrapod motor systems, but the underlying genetic mechanisms governing their formation has remained elusive. We found that *Pbx* genes are essential for the formation and differentiation of spinal motor columns. Consistent with roles as Hox cofactors, *Pbx* genes are required for the specification of MN subtypes along the rostrocaudal axis and the establishment of appropriate patterns of peripheral innervation. Unexpectedly, our study found that *Pbx* genes are also critical for the coalescence of MNs into columns, revealing a novel molecular program mediating the partitioning of dorsally projecting MMC neurons from all other MN subtypes. These studies could provide a foundation for resolving the role of MN position in locomotor circuit connectivity and exploring the origins of topographic organization within motor systems.

Pbx Genes as Cofactors for Hox-Dependent Steps in MN Differentiation

Hox genes are essential for the specification of neuronal classes along the rostrocaudal axis, where they contribute to the diversification and connectivity of MN columnar, divisional, and pool subtypes. Pbx cofactors are well known to enhance the affinity and binding selectivity of Hox proteins to target sites, but their precise roles during neuronal subtype specification are poorly defined. In the hindbrain, mutation of *Pbx* genes disrupts expression of extrinsic signaling factors, leading to non-cell-autonomous defects in neuronal specification and connectivity (Cooper et al., 2003; Vitobello et al., 2011). By eliminating *Pbx* genes selectively from MNs, we found that Pbx proteins are cell autonomously required for the differentiation of limb- and thoracic-specific MN subtypes. In contrast to the role of the Hox accessory factor Foxp1, which is necessary for subtype differentiation of LMC and PGC neurons (Dasen et al., 2008; Rousso et al., 2008), loss of *Pbx* genes affects all ventrally projecting MN subtypes. These results indicate that *Pbx* genes are essential for the differentiation of the majority of Hox-dependent subtypes.

While *Pbx* genes are necessary for the differentiation of MNs, not all Hox activities are lost in their absence. In spinal MNs, Hox cross-repressive interactions define the positions of columns and pools along the rostrocaudal axis, as exemplified by the phenotype of *Hoxc9* mutants, where brachial-level *Hox* genes are derepressed and thoracic MNs are transformed to an LMC fate (Jung et al., 2010). We found that *Pbx* genes are dispensable for this repressive activity, as in their absence *Hox* boundaries were preserved. Moreover, expression of the majority of *Hox* genes was not affected by the loss of *Pbx* genes, suggesting positive autoregulatory interactions are not critical in most spinal MNs. Thus, while the ability of *Hox* genes to promote neuronal diversity relies on *Pbx* activity, early Hox patterns appear to be established in a Pbx-independent manner.

Hox-Independent Roles of *Pbx* Genes in MN Columnar Organization

In tetrapods, MNs projecting to functionally related peripheral targets cluster into columnar and pool groups, establishing a central somatotopic map of peripheral innervation (Kania, 2014; Levine et al., 2012). The topographical organization of MNs can be revealed at a molecular level by the expression of certain classes of transcription factors, including Hox, Lim HD, and Foxp1 proteins (Dasen et al., 2008; Tsuchida et al., 1994). While Lim HD proteins define many MN subtypes, their specific role in establishing columnar organization is unclear. In mice lacking Lhx3/4 and Isl1/2 Lim HD proteins, MNs lose basic

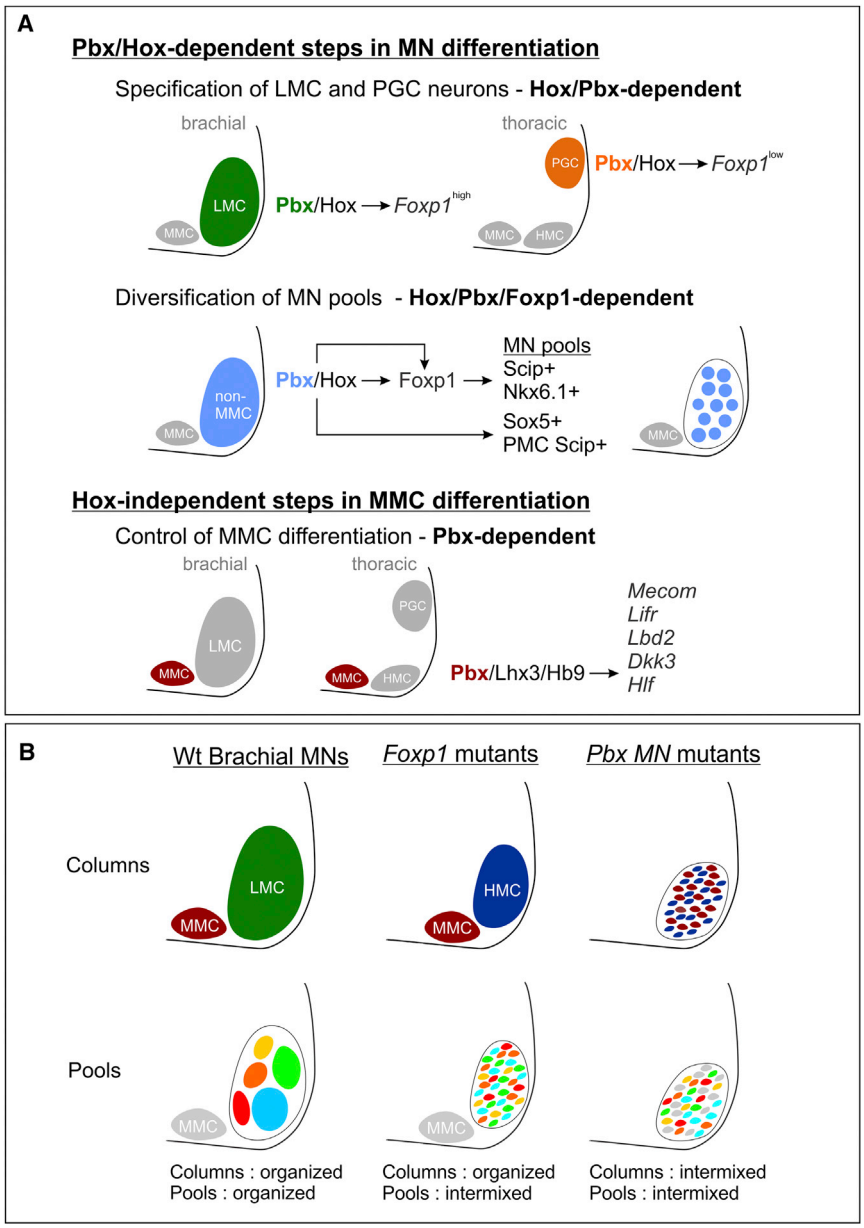

Figure 8. *Pbx* Genes Function in Parallel MN Differentiation Pathways

(A) *Pbx* genes are essential for Hox-dependent and -independent steps in MN differentiation. *Pbx* genes are required for two critical Hox-dependent steps: the specification of LMC and PGC columnar subtypes, and the diversification of LMC motor pools. *Pbx* genes are also necessary for the maturation of MMC neurons, and they govern the expression of a subset of MMC-restricted genes, including *Mecom*.

(B) Summary of defects in MN organization in *Foxp1* and *Pbx* mutants at brachial levels. MN organization in wild-type (WT) mice at brachial levels is shown. In *Foxp1* mutants, LMC neurons revert to an HMC-like identity but are clustered and segregated from MMC neurons. However, the position of MN pools projecting to individual muscles is disordered. In *Pbx* mutants, the remaining HMC and MMC neurons are intermixed, leading to severe defects in MN clustering.

features of their identity or are transformed to an interneuron fate (Sharma et al., 1998; Thaler et al., 2004), confounding any potential role in MN clustering. In the absence of *Hox* genes or *Foxp1*, MNs still retain core features of their identity, and the remaining columnar subtypes are well clustered. In contrast, *Pbx* genes appear to have a relatively specific role in segregating MMC from non-MMC populations. In the absence of *Pbx* genes, MNs still retain general features of their identity, but the remaining MMC and HMC populations are intermixed. These observations indicate that pathways acting within MMC and non-MMC populations ensure MN coalescence and appropriate settling position (Figure 8A).

In principle, the segregation of MMC and non-MMC populations could be governed by specific molecular programs acting within these groups or a consequence of the migratory paths of MNs as a function of their relative birth order. Our analysis of Pbx gene targets suggests the absence of columnar organization is due to the combined loss of molecular signatures of MMC and non-MMC neurons. We found that *Pbx* genes are essential to regulate a set of MMC-restricted genes, including the transcription factor *Mecom*. *Mecom* is selectively lost in *Pbx* mutants but retained in the absence of *Foxp1*, suggesting *Mecom* is regulated independently of Hox protein activity. Consistent with this idea, misexpression of determinants of MMC fates, such as Lhx3, can induce expression of *Mecom* at all rostrocaudal levels. Lhx3 is known to suppress Hox-dependent programs in MNs (Dasen et al., 2008), providing further evidence that *Mecom* induction does not rely on specific Hox proteins. In the cortex, a CNS region that lacks *Hox* gene expression, Pbx1 recently has been shown to bind within regions of the *Mecom* locus, suggesting direct regulation of *Mecom* by Pbx proteins (Golonzhka et al., 2015). These observations are in agreement with studies in *Drosophila* and mice, showing Pbx proteins have essential functions independent of their roles as Hox cofactors (Merabet and Mann, 2016). Our studies indicate that Pbx proteins can act within a single neuronal class to facilitate both Hox-dependent and Hox-independent programs of neuronal organization and connectivity.

MN Clustering and Topographic Organization within the Motor System

While multiple classes of transcription factors contribute to the formation of MN topographical maps, the developmental

mechanisms through which columnar organization is achieved are not well understood. *Reelin* and its receptor *Disabled* play essential roles in the migration and final positioning of LMC and PGC subtypes and are downstream targets of Foxp1 and Lhx1 (Palmesino et al., 2010). In mice lacking *Reelin* or *Disabled*, neurons occupy inappropriate positions within the spinal cord but are otherwise well clustered (Kania, 2014). The transcription factor Pea3 is necessary for the organization of MNs targeting the cutaneous maximus (CM) muscle, and, in *Pea3* mutants, CM neurons are interspersed with MN pools occupying the same segment. Targets of Pea3 include *cadherin8*, and type II cadherins have been implicated in the clustering of MN pools (Demireva et al., 2011; Livet et al., 2002). However, the early genetic pathways that ensure the clustering and segregation of MMC and non-MMC neurons are not known.

Our results indicate that *Pbx* genes operate in parallel pathways to govern MMC and non-MMC differentiation and that these two programs coordinate the coalescence and organization of motor columns. In non-MMC neurons, including limb-innervating LMC populations, loss of *Pbx* genes prevents the differentiation of Hox-dependent divisional and motor pool subtypes. These phenotypes are highly reminiscent of mutation in the Hox accessory factor *Foxp1*, where LMC neurons are transformed to an HMC fate and the position of LMC pools is scrambled, likely as a consequence of altered *cadherin* expression (Figure 8B). Nevertheless the segregation of MMC and HMC neurons persists in *Foxp1* mutants, due to the preservation of organizational systems acting within MMC neurons.

In *Pbx* mutants there is a selective depletion in a subset of MMC-restricted genes, and loss of these factors likely contributes to their disorganization. Importantly, loss of the Pbx-dependent program does not affect the ability of the remaining MMC and HMC neurons to select appropriate muscle targets, suggesting a unique function of Pbx targets in governing MN columnar organization. It is unlikely that this MMC-specific program governs MN coalescence alone, but rather it acts in concert with the Pbx/Hox-dependent network. Consistent with this idea, a preliminary analysis of existing *Mecom* mutants indicated a grossly normal segregation of MMC and non-MMC neurons (O.H., unpublished data), likely due to the preservation of Hox-dependent clustering programs. The disordering of MMC and non-MMC neurons therefore appears to be due to the loss of both Pbx-dependent programs, a condition that is achieved through the removal of *Pbx* genes from all MN subtypes.

Columnar Organization and the Evolution of Motor Circuits

What is the purpose of organizing MNs into columns? The segregation of MNs into columnar groups appears to be a unique organizational feature of vertebrates, and it is conserved in all tetrapod classes that have been examined, including birds, reptiles, and mammals (Jung and Dasen, 2015). A basic step in establishing MN topography involves the separation of dorsally projecting MMC neurons from ventrally projecting subtypes. In contrast, MNs targeting dorsal and ventral axial muscle compartments in zebrafish are largely intermixed with each other (Ampatzis et al., 2013; Menelaou and McLean, 2012). Nevertheless, axial MNs of zebrafish appear to be functionally organized along the dorsoventral axis, where specific groups of MMC-like neurons are recruited at distinct locomotor speeds (Ampatzis et al., 2014; McLean et al., 2007). This organizational feature may have evolved to coordinate the activation of axial MNs that drive specific types of undulatory locomotor behaviors, such as slow swimming or predator escape responses. In contrast, in tetrapods, MMC neurons are typically associated with postural stabilization, and locomotion is driven predominantly by LMC neurons. Although the origin of the Pbx-dependent MMC program in tetrapods is unclear, it may have appeared during the transition of vertebrates to terrestrial habitats, or it was selectively lost in lineages adapted to undulatory forms of locomotion.

The organization of MNs into columnar groups could impact the assembly and function of motor networks by restricting the neuronal populations to which a MN has access. It has been demonstrated that LMC and MMC neurons engage distinct populations of spinal premotor interneurons (Goetz et al., 2015). LMC neurons receive a preponderance of inputs from ipsilaterally located inhibitory interneurons, while MMC neurons connect with premotor populations that are evenly distributed across both sides of the spinal cord. The medial location of MMC neurons could enable access to the contralateral side of the spinal cord, allowing the MMC to capture a greater proportion of inputs from commissural interneurons. Similarly, the inputs that MNs receive from proprioceptive sensory neurons appear to be shaped by the relative position of motor pools within the LMC (Sürmeli et al., 2011). The Pbx-dependent pathways described here may have evolved as a means to separate MMC premotor circuits required for postural stabilization from the LMC-directed networks that govern locomotion.

EXPERIMENTAL PROCEDURES

Mouse Genetics

Pbx1 flox (Koss et al., 2012), *Pbx3*$^{-/-}$ (Rhee et al., 2004), and *Pbx3 flox* (Rottkamp et al., 2008) mice have been described previously. *Pbx3 flox* and *Hb9::eGFP* mice were obtained from The Jackson Laboratory. Animal procedures were performed in accordance with the NIH Animal Protection Guidelines and approved by the Institutional Animal Care and Use Committee of the New York University School of Medicine.

Whole Mount, Immunohistochemistry, and In Situ Hybridization

Immunohistochemistry was performed on 16-μm cryostat sections as described (Dasen et al., 2005). Primary antibodies were generated as described (Dasen et al., 2005, 2008; Tsuchida et al., 1994). Additional antibodies are described in the Supplemental Experimental Procedures. Whole-mount antibody staining was performed as described (Dasen et al., 2008), and GFP-labeled motor axons were visualized in projections of confocal z stacks (400–600 μm). Dissections and whole mounts of diaphragm muscles from E14–18.5 mice were stained as described (Philippidou et al., 2012). Unless indicated otherwise, immunohistological data shown in figures are representative of n > 3 mutants analyzed and are taken from animals that are *Pbx1*$^{MN\Delta}$;*Pbx3*$^{-/-}$. Images for control animals are from age-matched littermates that are Cre^{-} and either *Pbx3*$^{+/+}$ or *Pbx3*$^{+/-}$. Further information on histological analyses is given in the Supplemental Experimental Procedures.

In Ovo Chick Embryo Electroporation

Chick neural tube electroporations were performed at Hamburger and Hamilton (HH) st12–14 and analyzed at st27–28 as previously described (Dasen et al., 2003). Plasmid concentrations ranged from 100–500 ng/μl and pBKS was used as carrier DNA to achieve a final concentration of 1 μg/μl. Results

for each experiment are representative of five or more embryos in which the electroporation efficiency in MNs was >50%. The *Hoxc9IM-pCAGGS* construct was generated by mutation in the conserved Pbx interaction domain (ANWI→AAAI), and *Hoxc6IM-pCAGGS* has been described previously (Lacombe et al., 2013).

RNA-Seq and Computational Analysis

Details on the acquisition of RNA-seq data are given in the Supplemental Experimental Procedures. The alignment program, Bowtie (version 1.0.0), was used with reads mapped to the Ensemble NCBIM37/mm9 (iGenome version) with two mismatches allowed. The uniquely mapped reads were subjected to subsequent necessary processing, including removal of PCR duplicates, before transcripts were counted with htseq-count. Count files were imported into the R statistical programming environment and analyzed with the DESeq2 R/Bioconductor package (Love et al., 2014). Analyses were done on the NYULMC high-performance computing cluster. Reproducible pipeline scripts are available at https://github.com/dasenlab/Pbx-Neuron-Paper.

ACCESSION NUMBERS

The accession number for the RNA-seq data reported in this paper is GEO: GSE84271.

SUPPLEMENTAL INFORMATION

Supplemental Information includes Supplemental Experimental Procedures, seven figures, and three tables and can be found with this article online at http://dx.doi.org/10.1016/j.neuron.2016.07.043.

AUTHOR CONTRIBUTIONS

O.H. and J.S.D. conceived the project, designed the experiments, and wrote the paper. R.Z. and L.S. generated *Pbx* mutants, shared them prior to publication, and helped us recover lost lines after superstorm Sandy. L.J.C. and O.H. analyzed RNA-seq data. O.H., H.J., J.L., P.P., and D.H.L. performed experiments. All authors read and approved the final manuscript.

ACKNOWLEDGMENTS

We thank Myungin Baek, Gord Fishell, Holger Knaut, Hyung Don Ryoo, Brett Spurrier, and Hynek Wichterle for feedback and advice. We thank NYULMC's Office of Collaborative Science Cytometry core for FACS; the Rodent Genetic Engineering Core for mouse rederivation; and the Genomics Technology Core (GTC) for RNA-seq library preparation, sequencing, and bioinformatics. The GTC is partially supported by the Cancer Center Support Grant, P30CA016087, at the Laura and Isaac Perlmutter Cancer Center. The Bioinformatics core is supported in part by grant UL1 TR00038 from the NIH National Center for Advancing Translational Sciences (NCATS). L.S. is supported by National Institute of Dental and Craniofacial Research (NIDCR) R01 DE024745 and J.S.D. is supported by National Institute of Neurological Disorders and Stroke (NINDS) R01 NS062822 and R01 NS097550.

Received: February 4, 2016
Revised: June 20, 2016
Accepted: July 14, 2016
Published: August 25, 2016

REFERENCES

Ampatzis, K., Song, J., Ausborn, J., and El Manira, A. (2013). Pattern of innervation and recruitment of different classes of motoneurons in adult zebrafish. J. Neurosci. *33*, 10875–10886.

Ampatzis, K., Song, J., Ausborn, J., and El Manira, A. (2014). Separate microcircuit modules of distinct v2a interneurons and motoneurons control the speed of locomotion. Neuron *83*, 934–943.

Baek, M., and Mann, R.S. (2009). Lineage and birth date specify motor neuron targeting and dendritic architecture in adult Drosophila. J. Neurosci. *29*, 6904–6916.

Catela, C., Shin, M.M., Lee, D.H., Liu, J.P., and Dasen, J.S. (2016). Hox proteins coordinate motor neuron differentiation and connectivity programs through Ret/Gfrα genes. Cell Rep. *14*, 1901–1915.

Cooper, K.L., Leisenring, W.M., and Moens, C.B. (2003). Autonomous and nonautonomous functions for Hox/Pbx in branchiomotor neuron development. Dev. Biol. *253*, 200–213.

Dasen, J.S., Liu, J.P., and Jessell, T.M. (2003). Motor neuron columnar fate imposed by sequential phases of Hox-c activity. Nature *425*, 926–933.

Dasen, J.S., Tice, B.C., Brenner-Morton, S., and Jessell, T.M. (2005). A Hox regulatory network establishes motor neuron pool identity and target-muscle connectivity. Cell *123*, 477–491.

Dasen, J.S., De Camilli, A., Wang, B., Tucker, P.W., and Jessell, T.M. (2008). Hox repertoires for motor neuron diversity and connectivity gated by a single accessory factor, FoxP1. Cell *134*, 304–316.

Demireva, E.Y., Shapiro, L.S., Jessell, T.M., and Zampieri, N. (2011). Motor neuron position and topographic order imposed by β- and γ-catenin activities. Cell *147*, 641–652.

Fetcho, J.R. (1987). A review of the organization and evolution of motoneurons innervating the axial musculature of vertebrates. Brain Res. *434*, 243–280.

Goetz, C., Pivetta, C., and Arber, S. (2015). Distinct limb and trunk premotor circuits establish laterality in the spinal cord. Neuron *85*, 131–144.

Golonzhka, O., Nord, A., Tang, P.L., Lindtner, S., Ypsilanti, A.R., Ferretti, E., Visel, A., Selleri, L., and Rubenstein, J.L. (2015). Pbx regulates patterning of the cerebral cortex in progenitors and postmitotic neurons. Neuron *88*, 1192–1207.

Haase, G., Dessaud, E., Garcès, A., de Bovis, B., Birling, M., Filippi, P., Schmalbruch, H., Arber, S., and deLapeyrière, O. (2002). GDNF acts through PEA3 to regulate cell body positioning and muscle innervation of specific motor neuron pools. Neuron *35*, 893–905.

Hinckley, C.A., Alaynick, W.A., Gallarda, B.W., Hayashi, M., Hilde, K.L., Driscoll, S.P., Dekker, J.D., Tucker, H.O., Sharpee, T.O., and Pfaff, S.L. (2015). Spinal locomotor circuits develop using hierarchical rules based on motorneuron position and identity. Neuron *87*, 1008–1021.

Jung, H., and Dasen, J.S. (2015). Evolution of patterning systems and circuit elements for locomotion. Dev. Cell *32*, 408–422.

Jung, H., Lacombe, J., Mazzoni, E.O., Liem, K.F., Jr., Grinstein, J., Mahony, S., Mukhopadhyay, D., Gifford, D.K., Young, R.A., Anderson, K.V., et al. (2010). Global control of motor neuron topography mediated by the repressive actions of a single hox gene. Neuron *67*, 781–796.

Jung, H., Mazzoni, E.O., Soshnikova, N., Hanley, O., Venkatesh, B., Duboule, D., and Dasen, J.S. (2014). Evolving Hox activity profiles govern diversity in locomotor systems. Dev. Cell *29*, 171–187.

Kania, A. (2014). Spinal motor neuron migration and the significance of topographic organization in the nervous system. Adv. Exp. Med. Biol. *800*, 133–148.

Koss, M., Bolze, A., Brendolan, A., Saggese, M., Capellini, T.D., Bojilova, E., Boisson, B., Prall, O.W., Elliott, D.A., Solloway, M., et al. (2012). Congenital asplenia in mice and humans with mutations in a Pbx/Nkx2-5/p15 module. Dev. Cell *22*, 913–926.

Lacombe, J., Hanley, O., Jung, H., Philippidou, P., Surmeli, G., Grinstein, J., and Dasen, J.S. (2013). Genetic and functional modularity of Hox activities in the specification of limb-innervating motor neurons. PLoS Genet. *9*, e1003184.

Lance-Jones, C., and Landmesser, L. (1981). Pathway selection by chick lumbosacral motoneurons during normal development. Proc. R. Soc. Lond. B Biol. Sci. *214*, 1–18.

Landgraf, M., Jeffrey, V., Fujioka, M., Jaynes, J.B., and Bate, M. (2003). Embryonic origins of a motor system: motor dendrites form a myotopic map in Drosophila. PLoS Biol. *1*, E41.

Landmesser, L. (1978a). The development of motor projection patterns in the chick hind limb. J. Physiol. *284*, 391–414.

Landmesser, L. (1978b). The distribution of motoneurones supplying chick hind limb muscles. J. Physiol. *284*, 371–389.

Levine, A.J., Lewallen, K.A., and Pfaff, S.L. (2012). Spatial organization of cortical and spinal neurons controlling motor behavior. Curr. Opin. Neurobiol. *22*, 812–821.

Livet, J., Sigrist, M., Stroebel, S., De Paola, V., Price, S.R., Henderson, C.E., Jessell, T.M., and Arber, S. (2002). ETS gene Pea3 controls the central position and terminal arborization of specific motor neuron pools. Neuron *35*, 877–892.

Love, M.I., Huber, W., and Anders, S. (2014). Moderated estimation of fold change and dispersion for RNA-seq data with DESeq2. Genome Biol. *15*, 550.

Mann, R.S., Lelli, K.M., and Joshi, R. (2009). Hox specificity unique roles for cofactors and collaborators. Curr. Top. Dev. Biol. *88*, 63–101.

McLean, D.L., Fan, J., Higashijima, S., Hale, M.E., and Fetcho, J.R. (2007). A topographic map of recruitment in spinal cord. Nature *446*, 71–75.

Menelaou, E., and McLean, D.L. (2012). A gradient in endogenous rhythmicity and oscillatory drive matches recruitment order in an axial motor pool. J. Neurosci. *32*, 10925–10939.

Merabet, S., and Mann, R.S. (2016). To be specific or not: the critical relationship between Hox and TALE proteins. Trends Genet. *32*, 334–347.

Moens, C.B., and Selleri, L. (2006). Hox cofactors in vertebrate development. Dev. Biol. *291*, 193–206.

Palmesino, E., Rousso, D.L., Kao, T.J., Klar, A., Laufer, E., Uemura, O., Okamoto, H., Novitch, B.G., and Kania, A. (2010). Foxp1 and lhx1 coordinate motor neuron migration with axon trajectory choice by gating Reelin signalling. PLoS Biol. *8*, e1000446.

Philippidou, P., and Dasen, J.S. (2013). Hox genes: choreographers in neural development, architects of circuit organization. Neuron *80*, 12–34.

Philippidou, P., Walsh, C.M., Aubin, J., Jeannotte, L., and Dasen, J.S. (2012). Sustained Hox5 gene activity is required for respiratory motor neuron development. Nat. Neurosci. *15*, 1636–1644.

Price, S.R., De Marco Garcia, N.V., Ranscht, B., and Jessell, T.M. (2002). Regulation of motor neuron pool sorting by differential expression of type II cadherins. Cell *109*, 205–216.

Rhee, J.W., Arata, A., Selleri, L., Jacobs, Y., Arata, S., Onimaru, H., and Cleary, M.L. (2004). Pbx3 deficiency results in central hypoventilation. Am. J. Pathol. *165*, 1343–1350.

Romanes, G.J. (1951). The motor cell columns of the lumbo-sacral spinal cord of the cat. J. Comp. Neurol. *94*, 313–363.

Rottkamp, C.A., Lobur, K.J., Wladyka, C.L., Lucky, A.K., and O'Gorman, S. (2008). Pbx3 is required for normal locomotion and dorsal horn development. Dev. Biol. *314*, 23–39.

Rousso, D.L., Gaber, Z.B., Wellik, D., Morrisey, E.E., and Novitch, B.G. (2008). Coordinated actions of the forkhead protein Foxp1 and Hox proteins in the columnar organization of spinal motor neurons. Neuron *59*, 226–240.

Selleri, L., Depew, M.J., Jacobs, Y., Chanda, S.K., Tsang, K.Y., Cheah, K.S., Rubenstein, J.L., O'Gorman, S., and Cleary, M.L. (2001). Requirement for Pbx1 in skeletal patterning and programming chondrocyte proliferation and differentiation. Development *128*, 3543–3557.

Selleri, L., DiMartino, J., van Deursen, J., Brendolan, A., Sanyal, M., Boon, E., Capellini, T., Smith, K.S., Rhee, J., Pöpperl, H., et al. (2004). The TALE homeodomain protein Pbx2 is not essential for development and long-term survival. Mol. Cell. Biol. *24*, 5324–5331.

Sharma, K., Sheng, H.Z., Lettieri, K., Li, H., Karavanov, A., Potter, S., Westphal, H., and Pfaff, S.L. (1998). LIM homeodomain factors Lhx3 and Lhx4 assign subtype identities for motor neurons. Cell *95*, 817–828.

Sharma, K., Leonard, A.E., Lettieri, K., and Pfaff, S.L. (2000). Genetic and epigenetic mechanisms contribute to motor neuron pathfinding. Nature *406*, 515–519.

Sockanathan, S., and Jessell, T.M. (1998). Motor neuron-derived retinoid signaling specifies the subtype identity of spinal motor neurons. Cell *94*, 503–514.

Sürmeli, G., Akay, T., Ippolito, G.C., Tucker, P.W., and Jessell, T.M. (2011). Patterns of spinal sensory-motor connectivity prescribed by a dorsoventral positional template. Cell *147*, 653–665.

Thaler, J.P., Lee, S.K., Jurata, L.W., Gill, G.N., and Pfaff, S.L. (2002). LIM factor Lhx3 contributes to the specification of motor neuron and interneuron identity through cell-type-specific protein-protein interactions. Cell *110*, 237–249.

Thaler, J.P., Koo, S.J., Kania, A., Lettieri, K., Andrews, S., Cox, C., Jessell, T.M., and Pfaff, S.L. (2004). A postmitotic role for Isl-class LIM homeodomain proteins in the assignment of visceral spinal motor neuron identity. Neuron *41*, 337–350.

Thor, S., and Thomas, J.B. (2002). Motor neuron specification in worms, flies and mice: conserved and 'lost' mechanisms. Curr. Opin. Genet. Dev. *12*, 558–564.

Tsuchida, T., Ensini, M., Morton, S.B., Baldassare, M., Edlund, T., Jessell, T.M., and Pfaff, S.L. (1994). Topographic organization of embryonic motor neurons defined by expression of LIM homeobox genes. Cell *79*, 957–970.

Tümpel, S., Wiedemann, L.M., and Krumlauf, R. (2009). Hox genes and segmentation of the vertebrate hindbrain. Curr. Top. Dev. Biol. *88*, 103–137.

Vitobello, A., Ferretti, E., Lampe, X., Vilain, N., Ducret, S., Ori, M., Spetz, J.F., Selleri, L., and Rijli, F.M. (2011). Hox and Pbx factors control retinoic acid synthesis during hindbrain segmentation. Dev. Cell *20*, 469–482.

Waskiewicz, A.J., Rikhof, H.A., and Moens, C.B. (2002). Eliminating zebrafish pbx proteins reveals a hindbrain ground state. Dev. Cell *3*, 723–733.

William, C.M., Tanabe, Y., and Jessell, T.M. (2003). Regulation of motor neuron subtype identity by repressor activity of Mnx class homeodomain proteins. Development *130*, 1523–1536.